

IN-FLIGHT CALIBRATION/VALIDATION OF THE ENVISAT/MWR

Obligis E.⁽¹⁾, Eymard L.⁽²⁾, Dorandeu J.⁽¹⁾, Mertz F.⁽¹⁾ and Y. Faugère⁽¹⁾

⁽¹⁾CLS, 8-10 rue Hermes, 31526 Ramonville St Agne, France, Email : obligis@cls.fr

⁽²⁾CETP, 10-12 avenue de l'Europe, 78140 Velizy, France, Email : eynard@cetp.ipsl.fr

ABSTRACT/RESUME

This paper presents the methodology used for the Envisat/MWR calibration as well as the performance concerning the level 2 radiometer products.

1 DATA USED

The data we used for this study are ERS2 and Envisat data for cycle 78 and 10 respectively. Selected measurements are only over ocean and without ice (we use the same editing criterion for Envisat and ERS2 products to filter the ice).

2 METHODOLOGY FOR THE MWR CALIBRATION

The retrieval algorithms have been formulated in 2001 using ECMWF analyses (4 analyses between summer 2000 and spring 2001), as well as simulations using a radiative transfer model, and a classical linear regression for the determination of the coefficients in the different algorithms.

Unfortunately there has been an important change in the ECMWF model in January 2002 and the calibration of the Envisat/MWR brightness temperatures if performed over 2002 analyses will not be consistent with the algorithms formulated over 2000/2001 analyses.

This is why we have decided to use ERS2 brightness temperatures adjusted to the 2000/2001 database as reference for the ENVISAT brightness temperatures. Figure 1 shows the scatterplots obtained in 2001 between ERS2 measurements and simulations by our radiative transfer model over coincident ECMWF fields. Biases (+4.91 K for the 23.8 GHz channel and 2.16 K for the 36.5 GHz channel) mean that an optimal behavior of the algorithms will be obtained when adding these bias values to the ERS2 measured brightness temperatures.

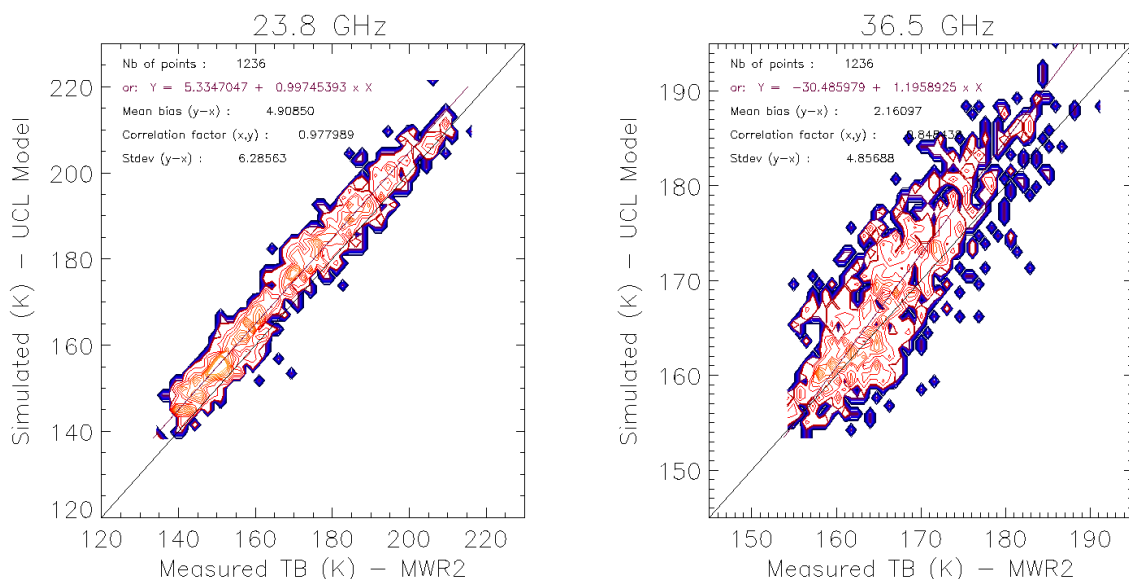


Figure 1

The calibration of the Envisat brightness temperatures has therefore been performed in order to get the best consistency between adjusted ERS2 brightness temperatures and calibrated Envisat brightness temperatures. Three parameters have been tuned at the instrument level to obtain this consistency. These 3 parameters are :

- η_{ref} coefficients : the initial values for this parameter were 0.984 at 23.8 GHz and 0.977 at 36.5 GHz. After a first adjustment to the ERS2 values, we propose a new modification : 0.99 at 23.8 GHz and 0.999 at 36.5 GHz.
- a_{cc} coefficients : the method consists in an iterative adjustment of the a_{cc} values in order to get gain values as closer as possible from the on ground values. The values we propose for the a_{cc} coefficients are 1.01 at 23.8 GHz and 1.04 at 36.5 GHz.
- c_1 coefficients : c_1 is the main antenna transmission coefficient and is defined by $c_1=1/(a_{feed} \cdot a_r)$, where a_{feed} is the main antenna feed transmission coefficient and a_r is the measurement antenna wave-guide transmission coefficient. As each of these 2 parameters are implied in other parameters, they have to be tuned simultaneously to adjust the c_1 coefficient. The new values for a_r are 0.979 (unchanged) at 23.8 GHz and 0.840 at 36.5 GHz. The new values for a_{feed} are 0.936 (unchanged) at 23.8 GHz and 0.840 at 36.5 GHz.

Table 1 contains a summary of the changes regarding the original values.

	23.8 GHz channel		36.5 GHz channel	
	Original	New	Original	New
η_{ref}	0.984	0.99	0.977	0.999
A_{cc}	1.028	1.01	1.039	1.04
A_r	0.979	0.979	0.959	0.840
a_{feed}	0.936	0.936	0.973	0.840
c_1	1.091	1.091	1.072	1.417

Table 1

3 CYCLE 10 BRIGHTNESS TEMPERATURES

Figures 2 and 3 show the histograms of cycle 10 Envisat brightness temperatures over ocean for the 2 channels. The form of both histograms is correct as well as associated statistical parameters.

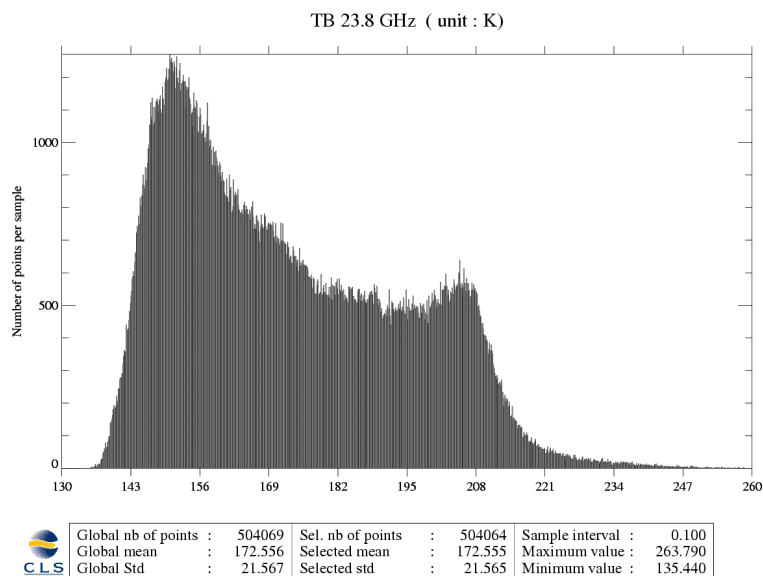


Figure 2

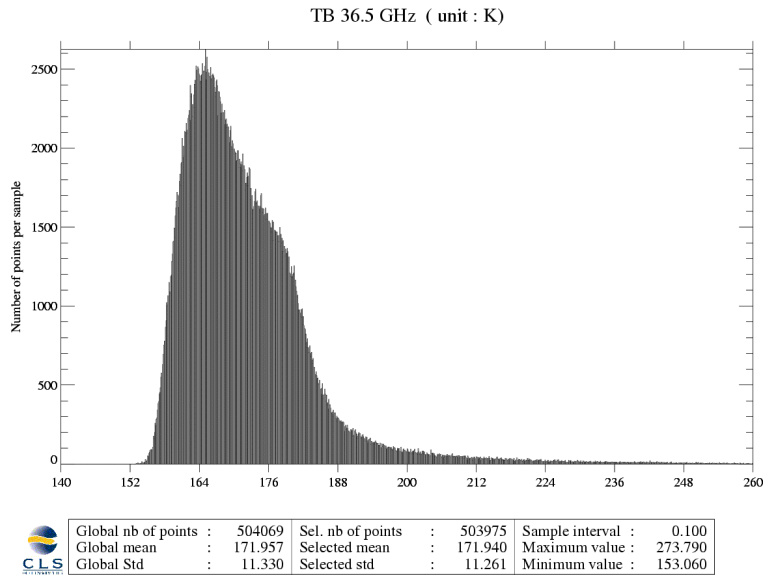


Figure 3

Figure 4 show the scatterplots obtained between ERS2 adjusted brightness temperatures (after adding the biases indicated in §2) and Envisat calibrated brightness temperatures.

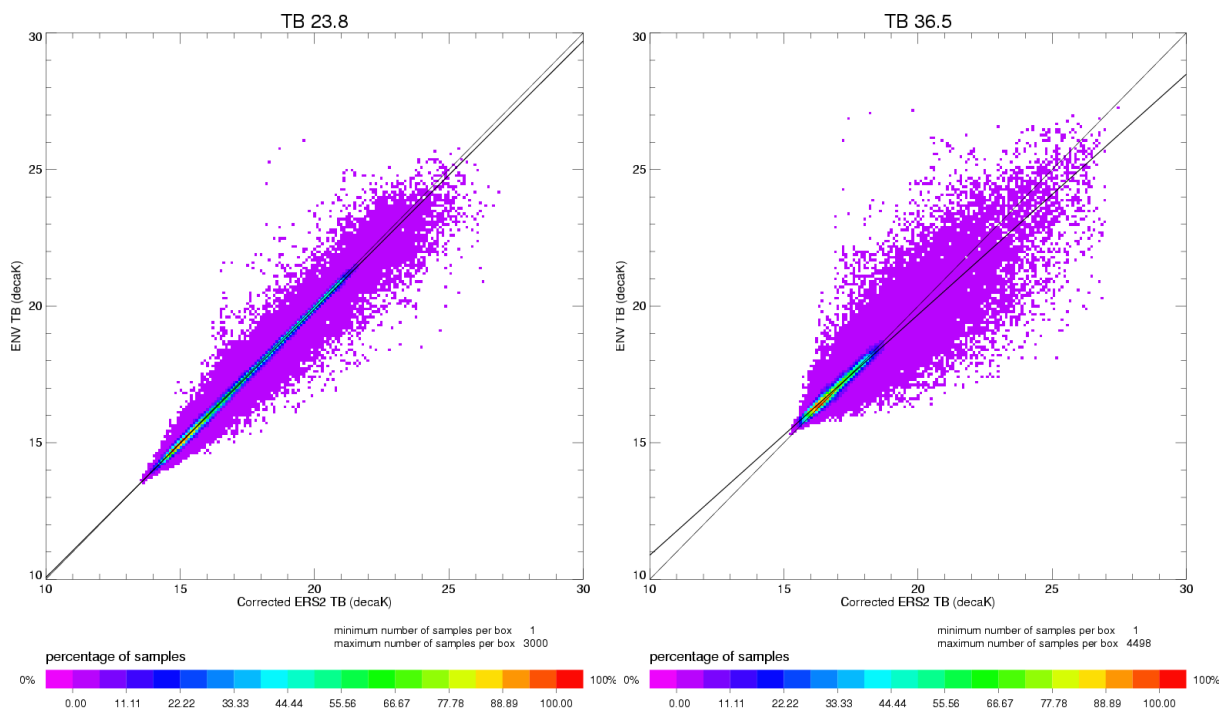


Figure 4

Results are satisfactory (biases lower than 1K), particularly for the first channel with a slope very closed to one. For the second channel, dispersion is higher due to the high variability in space and time of the cloud liquid water content.

4 CYCLE 10 LEVEL 2 PRODUCTS

All radiometer products are computed using log-linear algorithm of the form :

$$P = c0 + c1 * \ln(280 - TB23.8) + c2 * \ln(280 - TB36.5) + c3 / (\sigma_{0Ku}^2)$$

where P is the wet tropospheric correction, or the integrated water vapor content, or the integrated cloud liquid water content, or the atmospheric attenuation of the backscattering coefficient in Ku band, or of the backscattering coefficient in S band.

Figure 5 shows the histogram of σ_{0Ku} , when using the products. The mean value is around 8.8 dB. This value is more than 2 dB lower than the mean value obtained with TOPEX, POSEIDON, ERS1, and ERS2 altimeters.

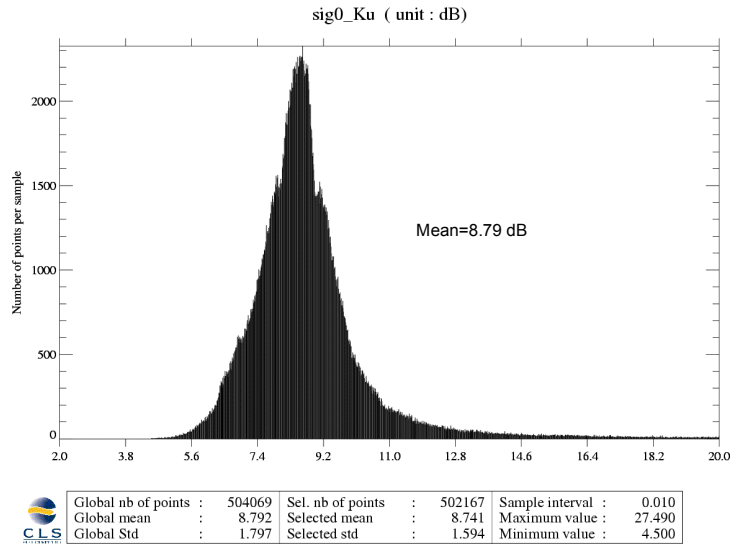


Figure 5

Figure 6 shows the scatterplot obtained by inter-comparison between ERS2 σ_{0Ku} and ENVISAT σ_{0Ku} . The difference is very closed to a bias, and the estimated value for this bias is 2.41 dB.

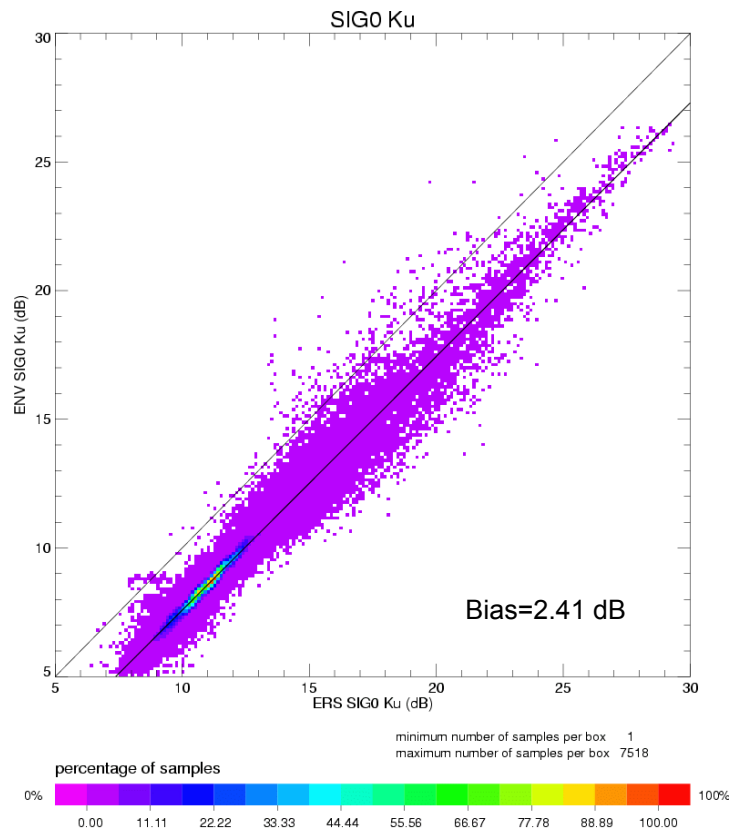


Figure 6

This too low value of the ENVISAT σ_{0Ku} has a direct impact on all radiometer products. This is illustrated on figure 7 for the wet tropospheric correction. The histogram shows a lot of negative values and a mean value for the cycle which is too low.

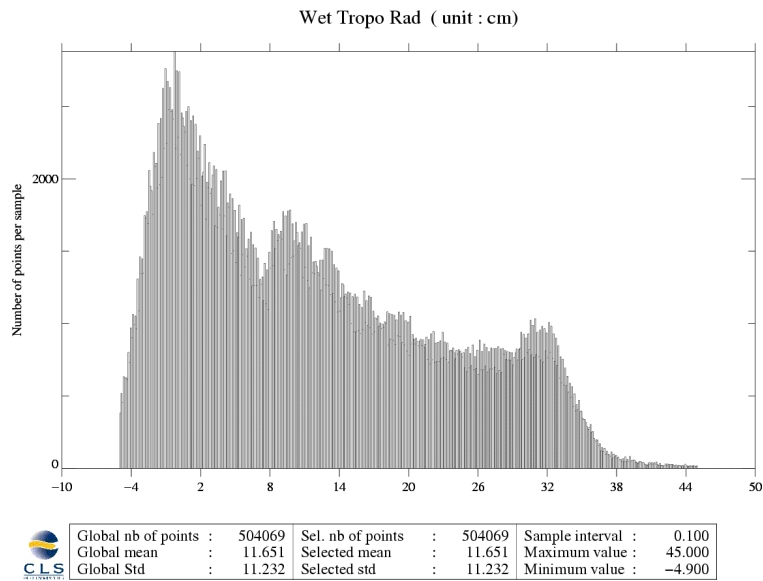


Figure 7

The scatterplot between ERS2 and ENVISAT wet tropospheric corrections is plotted on figure 8. As expected a bias on the σ_{0Ku} values does not imply only a bias on the wet tropospheric correction.

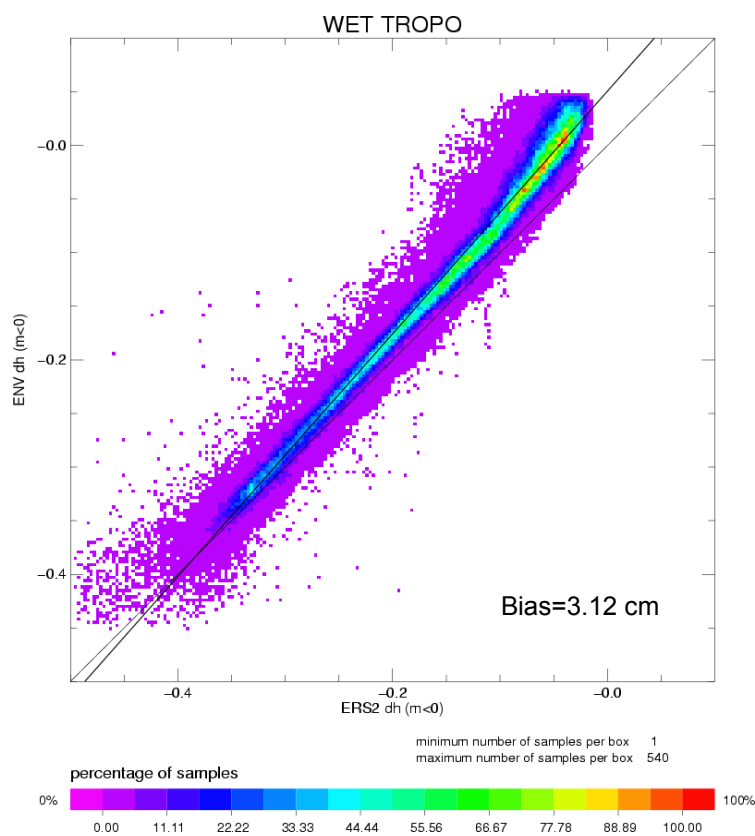


Figure 8

We have therefore adjusted the σ_{0Ku} values to get correct radiometer products, and evaluate the quality of these new products. The correction to be applied on the Envisat σ_{0Ku} in the product is the following :

- add 2.41 dB to get a σ_{0Ku} values consistent with the ERS2 ones
- add 1 dB more to provide σ_{0Ku} values closer to the ones simulated with our radiative transfer model (as recommended in the TN from October 2002)

A bias of 3.41 dB has been added to the product values and all radiometer geophysical products have been calculated again using these new values for σ_{0Ku} .

Figure 9 shows the new histogram for the wet tropospheric correction. The form is slightly different, the mean value is higher. It still remains some negative values (-2.3 mm) but this is no more critical.

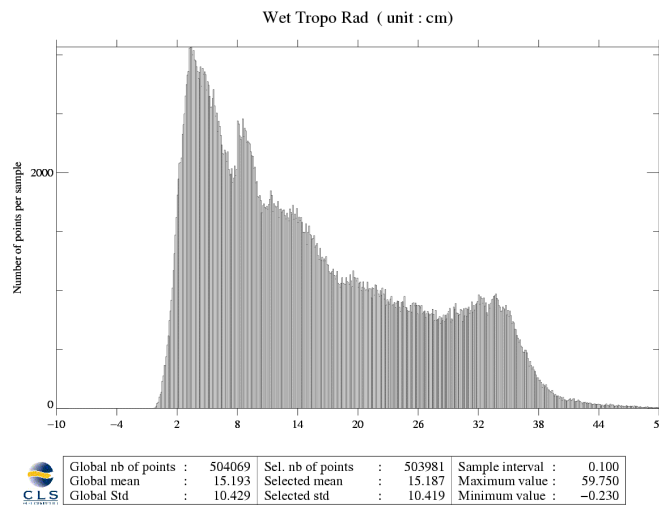


Figure 9

Figure 10 presents the new scatterplot between ERS2 and Envisat radiometer wet tropospheric corrections. The agreement between the two is satisfactory with a mean bias of 4.5 mm and a standard deviation of 10 mm. This scatterplot shows drier values for dry atmosphere (this feature is due to the linear correction added to the Envisat algorithm in case of $|dh| < 8\text{cm}$) and wetter values for wet atmosphere ($|dh| > 10\text{cm}$).

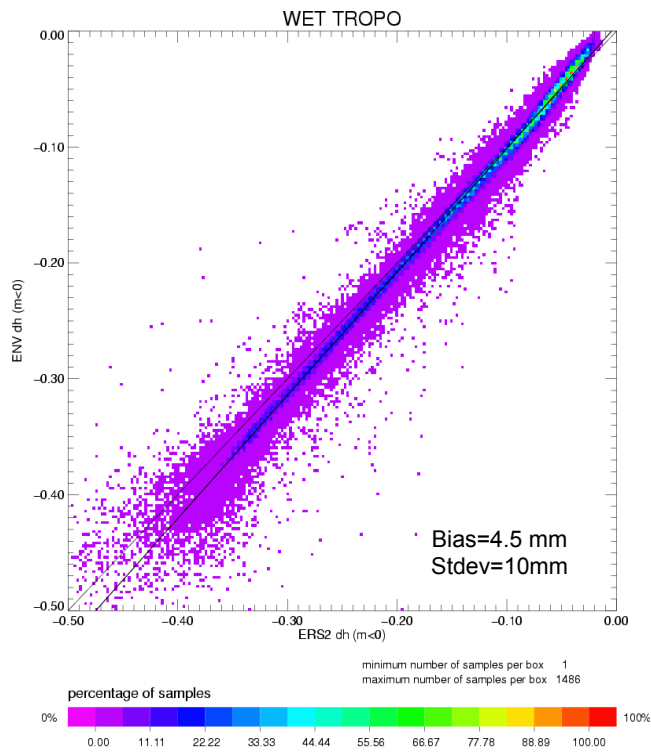


Figure 10

A similar scatterplot (with higher dispersion) is obtained when comparing ECMWF and Envisat wet tropospheric corrections : figure 11.

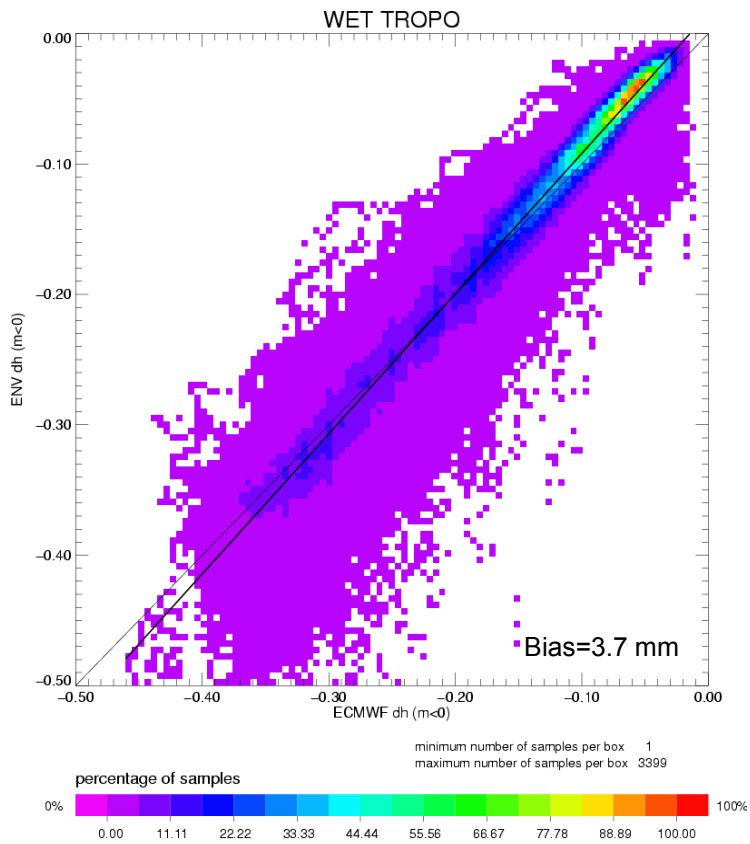


Figure 11

This positive value of bias between ERS2 and Envisat wet tropospheric corrections (4.5 mm) is satisfactory. Figure 12 shows the comparison between radiosounding and ERS2 wet tropospheric corrections for a 6 years period. This plot showed a systematic underestimation of the wet tropospheric (mean bias of -6.2 mm). Knowing that the Envisat wet tropospheric will be around 5mm higher than the ERS2 one, we will get a better agreement with radiosounding measurements.

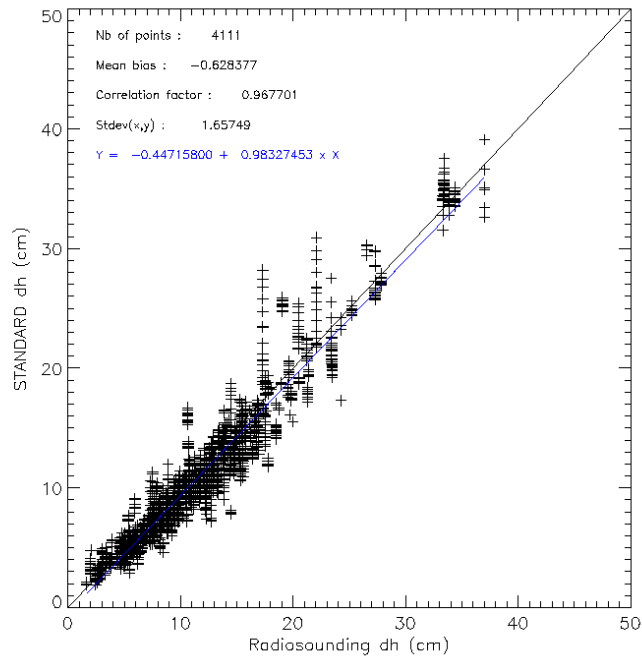


Figure 12

Figures 13 to 16 show respectively the histograms obtained for the integrated water vapor content, the integrated cloud liquid water content, the atmospheric attenuation of the backscattering coefficients in Ku and S band. The 4 histograms are satisfactory in terms of mean, minimum and maximum values. The only problem is the presence of negative values for the cloud water which is not critical. The accuracy for this algorithm is estimated to be around 0.05 kg.m^{-2} , so values between -0.05 and 0 are acceptable. The residual presence of values even lower should be solved with the new calibration of the 36.5 GHz channel (to be performed after the drift explanation/correction).

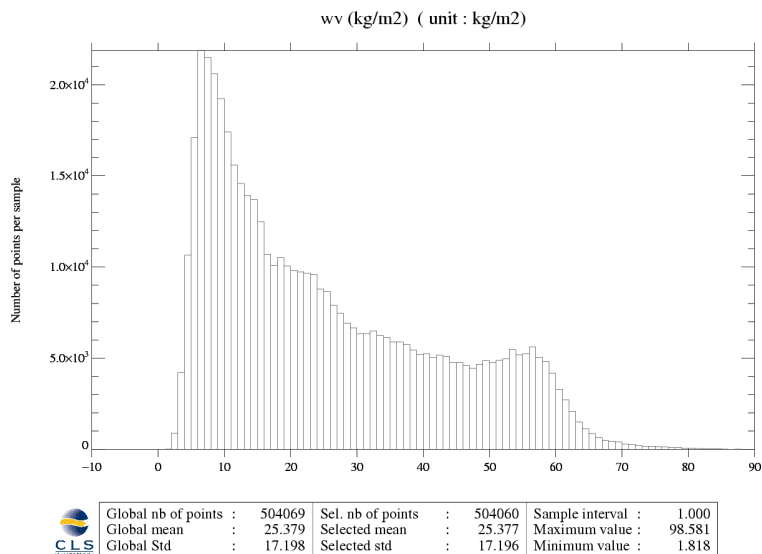


Figure 13

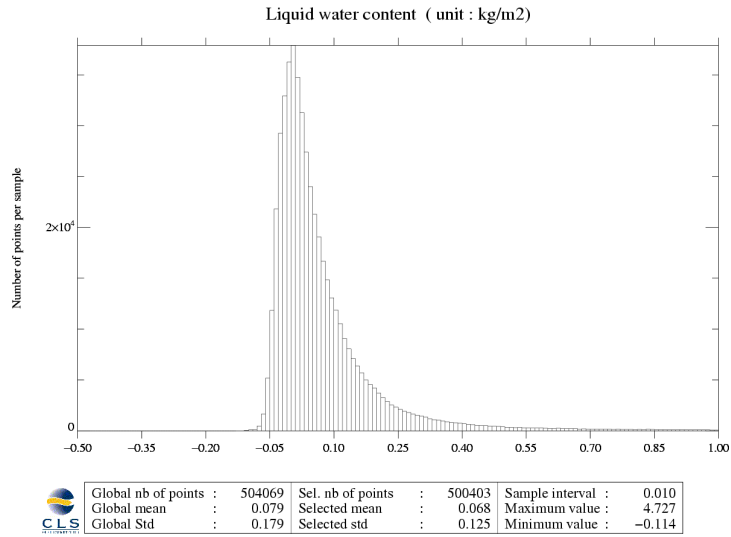


Figure 14

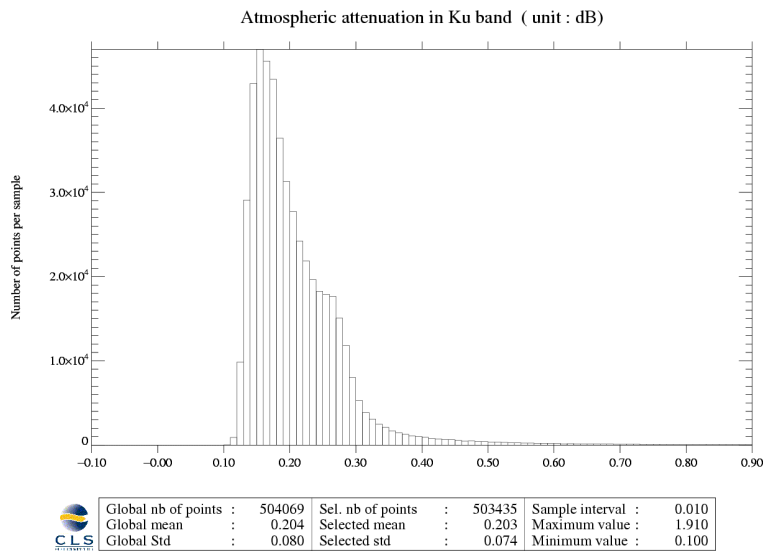


Figure 15

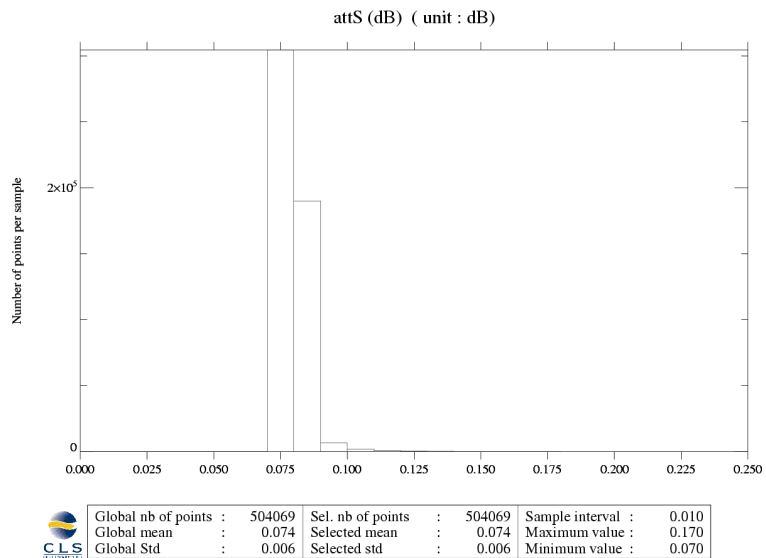


Figure 16

5 NEURAL NETWORK ALGORITHMS

Over the 2000/2001 database, we have formulated in parallel parametric and neural algorithms. The main advantage of a neural algorithm is that we do not need an a priori form for the algorithm. The “regression” is better performed particularly in the border of the domain. For example, in the particular case of the wet tropospheric correction, the linear correction added in case of dry atmosphere is no more necessary.

Figure 17 shows the scatterplot obtained between ERS2 dh and ENVISAT dh computed with a corrected σ_{0Ku} and a neural algorithm. This figure is very similar to figure 10 with a mean bias of 6.7mm.

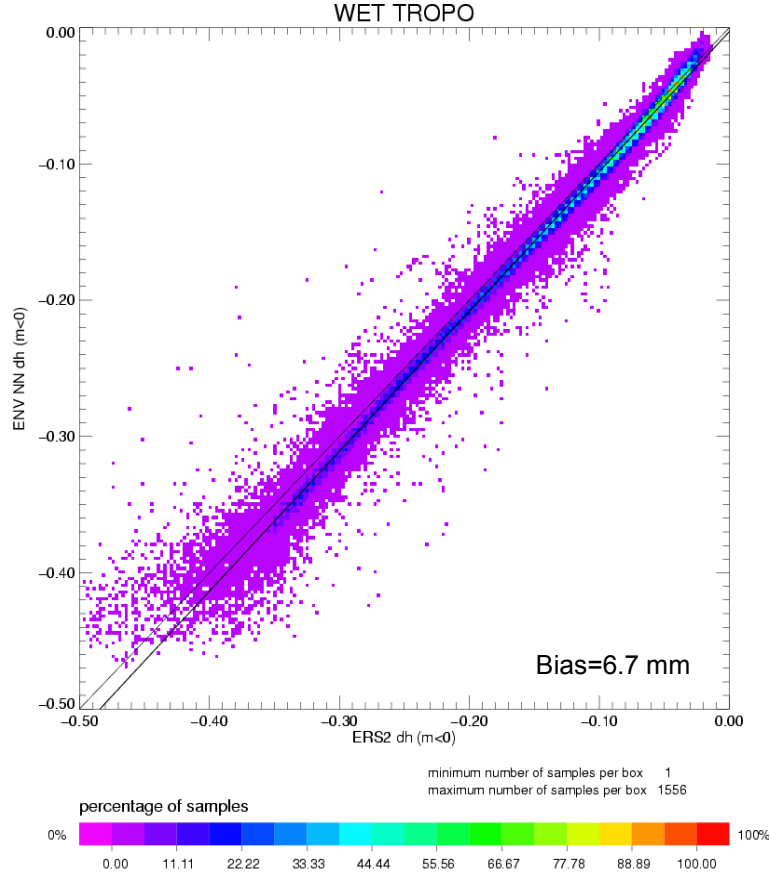


Figure 17

6 NEW SIDE LOBE ALGORITHM

The temperature measured by the radiometer T_A contains the contribution of the side lobe :

$$T_A = \eta_{glob} T_B + T_{slg}$$

with $\eta_{glob} = \eta_{refl} \times \eta_{ml}$

and $T_{slg} = \eta_{refl} \times T_{sl} + (1 - \eta_{refl}) \times T_{sl}$

where η_{refl} is the transmission coefficient of the reflector, η_{ml} is the antenna main lobes beam efficiency, T_B is the brightness temperature in the main lobe and T_{sl} is total secondary lobe contribution.

In the actual version of the level 1 processing chain, the contribution T_{sl} is considered constant (8.21K at 23.8 GHz and 0.413K at 36.5 GHz). The importance of this contribution for the first channel makes the use of a constant term a strong assumption. This is why we propose an improved algorithm considering a side lobe correction depending on the season and on the position of the pixel.

$$T_{sl} = \eta_{sun} \times T_{sun} + \eta_{sky} \times T_{sky} + \eta_{earth} \times T_{earth} + \eta_{sat} \times T_{sat}$$

η_{sun} is the efficiency of the side lobe aiming the sun, T_{sun} is the sun temperature ($\eta_{sun}=0$).

η_{sky} is the efficiency of the side lobe aiming the sky, T_{sky} is the sky temperature ($T_{sky}=2.73K$).

η_{sat} is the efficiency of the side lobe aiming the satellite, T_{sat} is the satellite temperature ($T_{sat}=T_{earth}$).

η_{earth} is the efficiency of the side lobe aiming the earth, T_{earth} is the earth temperature.

T_{earth} is estimated for each mesh of $1^\circ \times 1^\circ$ over the globe and for each season from one year of ERS2 brightness temperatures. Figure 18 shows the side lobe contribution obtained for the 23.8 GHz channel and for spring.

Side Lobe corrections at 24 GHz

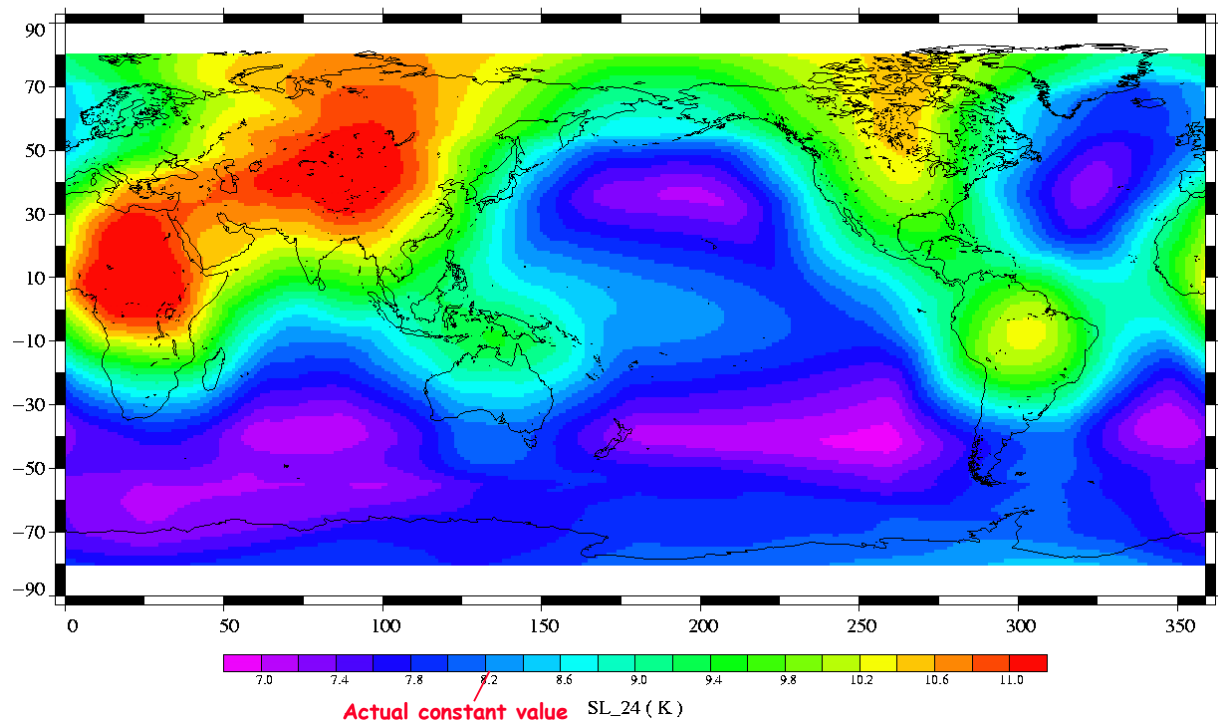


Figure 18

Figure 19 gives an illustration of the difference between 23.8 GHz brightness temperatures corrected with the new algorithm and brightness temperatures corrected with the operational one for cycle 10. The mean difference is very closed to zero, but significant differences appear in coastal regions (Guinea Golf, Mediterranean Sea...) or in deep ocean.

Difference between Side Lobe corrections at 24 GHz

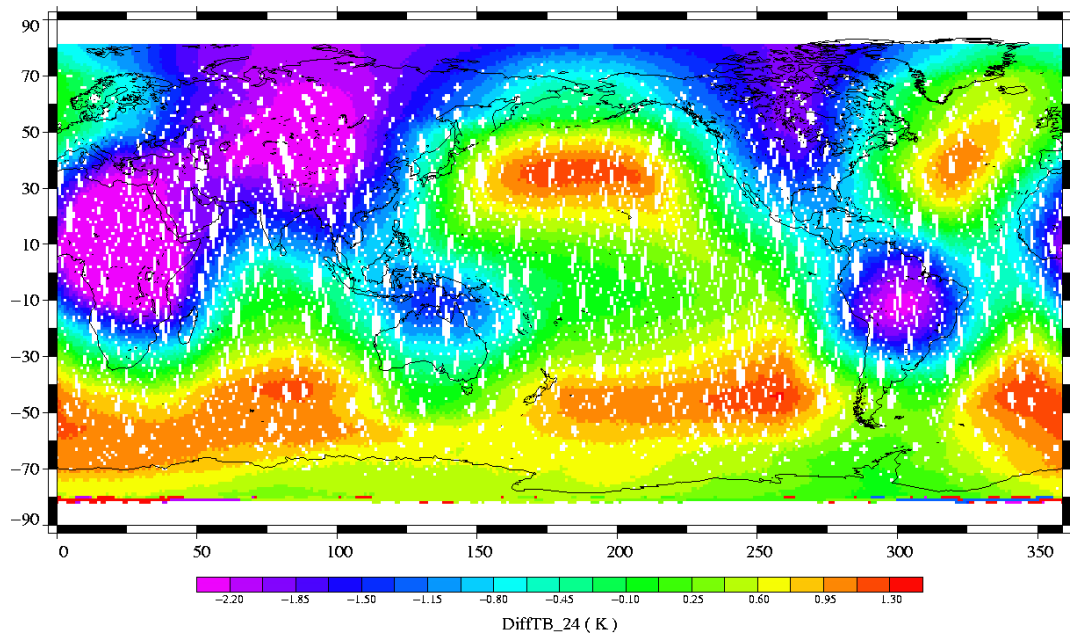


Figure 19

Figure 20 is the same for the 36.5 GHz channel. Due to the lower efficiency of the satellite in the side lobe, the approximation of a constant contribution is more valuable and the difference between the 2 algorithms is much lower ($<0.1K$).

Difference between Side Lobe corrections at 36 GHz

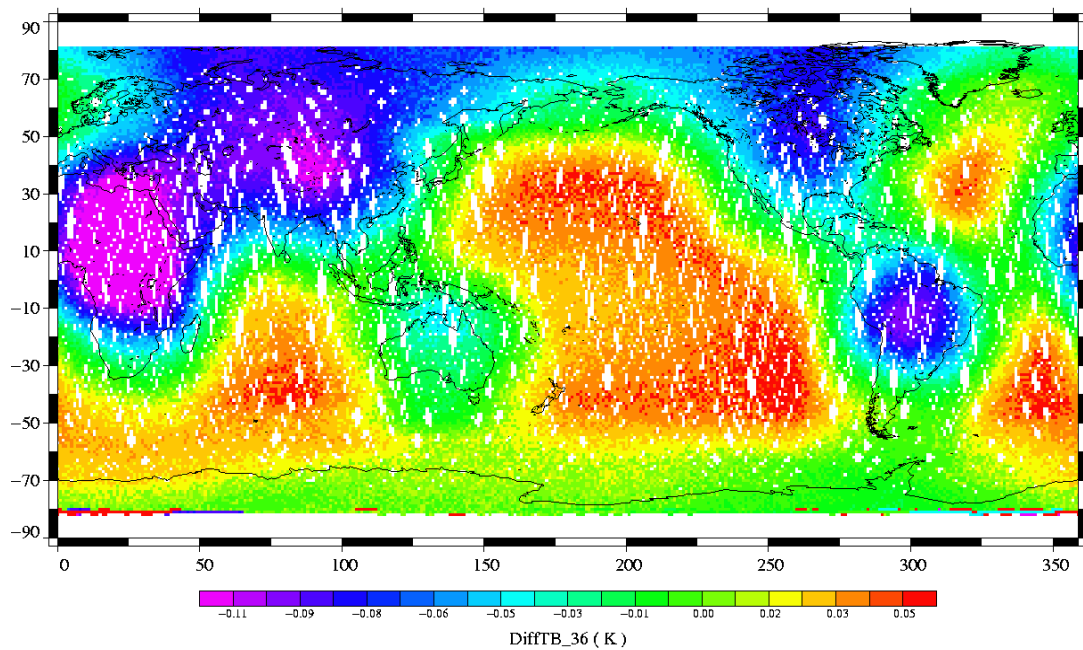


Figure 20

The impact of this new correction on the wet tropospheric correction is illustrated on figure 21 (scatterplot between dh computed from TBs corrected with a constant term and dh computed from TBs corrected using the new algorithm). The mean bias between the two is very low (0.7mm) but the standard deviation is 7 mm.

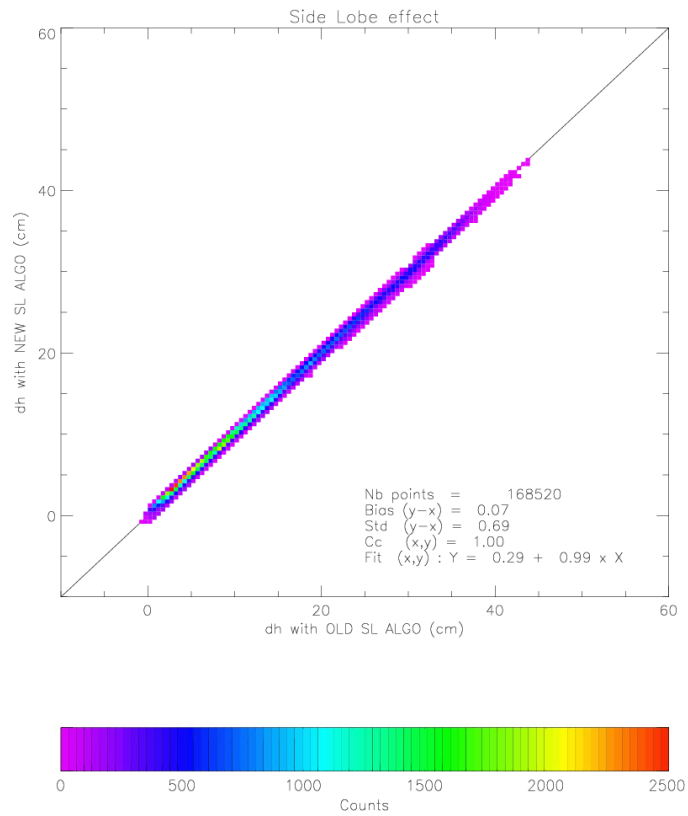


Figure 21

Figure 22 shows a cartography of the difference between the two dh values. The difference can reach 1cm in coastal areas. This means that this new correction has a significant impact on the wet tropospheric correction values and that this improvement has to be taken into account.

DH_NEWSL – DH_OLD (mm)

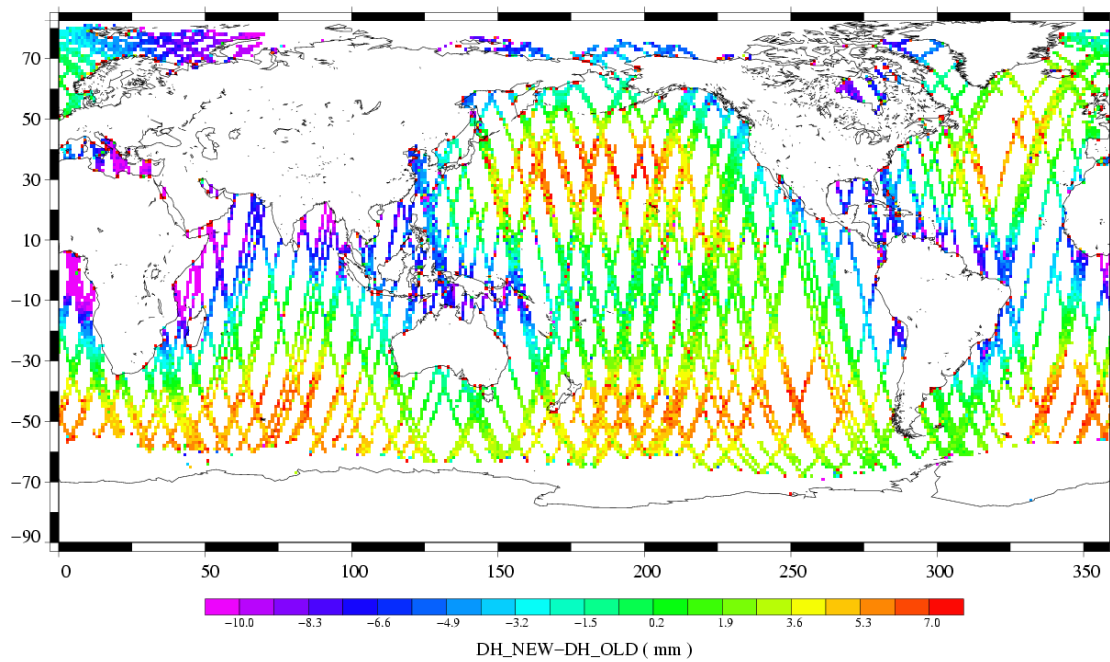


Figure 22

7 CONCLUSIONS/RECOMMENDATIONS

The Envisat/MWR has been calibrated to get consistency with the 2000/2001 database used for the computation of the different geophysical parameters.

To provide reliable Level 2 products we recommend a backscattering coefficient in Ku band 1 dB higher than the ERS2 one. The value used in input of the different radiometer algorithms should have a global value over sea around 12 dB.

With an appropriate value for the backscattering coefficient of the Ku band, we found a mean bias around 5 mm between Envisat and ERS2 wet tropospheric corrections (Envisat wetter). This will lead to a better agreement with radiosounding measurements.

The impact of the new side lobe correction algorithm we propose has been estimated (up to 1 cm near the coast). The validation of this algorithm is on the way.

Neural network algorithms have been formulated and are now ready for operational application.

The drift of the 36.5 GHz channel gain pointed out by the CETP has not been taken into account because the calibration performed over September data is still valuable for cycle 10.